Sustainable Food Technology

ROYAL SOCIETY OF CHEMISTRY

PAPER

View Article Online
View Journal | View Issue

Cite this: *Sustainable Food Technol.*, 2025, **3**, 1218

Valorization of grapevine agricultural waste into transparent and high-strength biodegradable films for sustainable packaging†

Sandeep Paudel,[a] Sumi Regmi,[a] Sajal Bhattarai,[ab] Anne Fennell[c] and Srinivas Janaswamy *[ac]

The impact of single-use and short-lived plastic food packaging is significant, contributing substantially to environmental waste that harms ecosystems. Microplastic pollution and chemical leaching from plastic packaging pose risks to humans, animals, and plants. Consequently, our environment is increasingly contaminated by plastic waste, microplastics, and nanoplastics, resulting in a pervasive pollutant. In this context, alternative biodegradable and sustainable packaging can help mitigate the harmful effects of plastic waste. Agricultural byproducts, which might otherwise be discarded, hold considerable potential for this purpose. This study demonstrates the use of grapevines as a source of cellulose to develop novel, transparent, and biodegradable films. Grapevine canes are major woody berry crops that generate substantial winter pruning waste. This waste contains a high level of cellulose, approximately 35%. Herein, the cellulose fraction was extracted using alkaline (10% KOH) and bleaching (10% $NaClO_2$) treatments. It was then solubilized in a $ZnCl_2$ solution, crosslinked with calcium ions, and plasticized with glycerol to develop films. These films exhibit a transparency of 83.70–84.30% mm^{-1} and a tensile strength of 15.42–18.20 MPa. They biodegrade within 17 days in soil at 24% moisture content. These films demonstrate outstanding potential for food packaging applications. Our research approach of repurposing agricultural byproducts to create high-value products helps reduce plastic waste, conserve the environment, and provide economic benefits to farmers.

Received 16th May 2025
Accepted 20th June 2025

DOI: 10.1039/d5fb00211g

rsc.li/susfoodtech

Sustainability spotlight

The widespread use of petroleum-based plastics continues to pose serious threats to the environment, impacting plant, animal, and human health. Therefore, there is an urgent need for sustainable alternatives. In an innovative step toward addressing this issue, this study explores the potential of an underutilized agricultural byproduct, the grapevine, as a renewable source of cellulose for developing biodegradable packaging. The cellulosic residue has been extracted from the grapevine, and environmentally friendly packaging films have been developed. These films are transparent, strong, and biodegrade within 17 days in soil moisture content of 24%, leaving no harmful residues behind. This rapid and safe breakdown highlights grapevine cellulose films as a highly promising material to replace conventional plastic packaging. By transforming agricultural waste into value-added materials, this research supports a circular economy and significantly contributes to the advancement of sustainable packaging solutions.

1. Introduction

Plastic packaging has become a vital component of modern life. Approximately 50% of all plastics produced are single-use,[1] typically having a short lifespan limited to the period of product consumption. Plastic production increases annually to meet global demand, with the packaging industry accounting for approximately 40% of usage.[2] Plastic materials are derived from fossil-based non-renewable resources and can persist in the environment for centuries due to their non-biodegradable nature, with recyclability of only 9%.[3,4] The resulting white pollution severely harms ecosystems and contributes to the deaths of thousands of animals from entanglement and ingestion.[5–9] Plastic breaks down into microplastics and nanoplastics, and these tiny particles can be ingested or inhaled by both animals and humans, posing significant health risks.[10–13] Biodegradable, non-toxic, and sustainable packaging alternatives are necessary to address these issues.[14–17] Several studies have explored the development of biodegradable packaging materials derived from starch, proteins, chitosan, pectin, and gums. However, cellulose stands out as the most abundant,

[a]*Department of Dairy and Food Science, South Dakota State University, Brookings, SD 57007, USA. E-mail: Srinivas.Janaswamy@sdstate.edu*

[b]*Department of Food Science, Purdue University, West Lafayette, IN 47907, USA*

[c]*Department of Agronomy, Horticulture and Plant Science, South Dakota State University, Brookings, SD 57007, USA*

† Electronic supplementary information (ESI) available. See DOI: https://doi.org/10.1039/d5fb00211g

strong, and stiff biopolymer. In this context, agricultural waste, which is rich in cellulose, presents a viable solution for designing and developing eco-friendly packaging materials.[18–22] Only a limited number of studies have investigated the extraction of cellulose from agricultural waste for the development of packaging films. Some of the examples include alfalfa,[23] soyhulls,[24] avocado peel,[25] banana peel,[26] rice husk,[27] and sugarcane bagasse.[27] Therefore, the present study aims to utilize the abundantly available grapevine waste as a source of cellulose for developing eco-friendly packaging films with the potential to replace petroleum-based plastics. This submission highlights the importance of grapevine canes for creating packaging films.

Grapevine canes are woody berry crops that produced 74.94 million metric tons of fruit in 2022.[28] They comprise 35% cellulose, 28% hemicellulose, and 29% lignin, along with proteins, fats, minerals, and bioactive compounds.[29] By extracting these biopolymers, value-added products can be created. Several high-value applications of winter grapevine pruning (WGVP), including particleboard, biofuel, biostimulants, composting, and activated carbon, are being explored.[30–34] Each year, a significant amount of WGVP is generated, ranging from 6.7 to 18.6 million metric tons.[35] The yield of cellulosic residue is estimated to be 2.4 to 6.5 million tons. However, a small portion is usually left in the vineyard to enhance soil nutrient quality, while the rest may be burned, contributing to global warming. A strategic approach to managing WGVP is crucial to mitigate its harmful environmental impact. Thus, utilizing grapevine waste to develop value-added products represents a sustainable and effective solution. Farmers spend around $26 per ton on disposing of grapevines. This expenditure can be saved by adding it to the processor's cost of $84–94 per ton.[36] This will result in annual savings of $174.2–483.6 million for farmers, and cellulosic residue costs around $240–268.6 per ton. In this research, 0.4 g of cellulosic residue yielded a 0.0144 m^2 film. Thus, 2.4 to 6.5 million tons of cellulosic residue would yield 86.4–234.0 billion square meters of film, at an estimated cost of $0.0067–0.0075 per square meter. This price is significantly lower than that of soy hull film ($0.0125)[24] and alfalfa cellulose film ($0.0178),[23] suggesting the potential of grapevine cellulose residue in creating biodegradable packaging films. However, a full-scale techno-economic analysis is necessary to accurately estimate the price, including cellulose extraction and other overhead costs.

Incorporating 10% WGVP into high-density polyethylene composites has improved tensile strength by 53%.[29] However, extracting cellulosic residue and creating biodegradable packaging films would be advantageous for developing alternatives to plastic-based packaging films. Indeed, cellulose decomposes in soil through microbial activity, resulting in harmless end products. Nonetheless, cellulosic residue derived from agricultural waste, agricultural biomass, and agro-processing byproducts would be more beneficial for designing and developing biodegradable packaging films, contributing to sustainability and the circular bioeconomy. A few successful examples include cellulosic residue from corncob,[37] soy hulls,[38,39] spent coffee grounds,[40] switchgrass,[41,42] wheat straw,[43] and oat straw.[44] The mechanical strength, moisture barrier, optical translucence, and biodegradation properties of the films vary depending on the source of the cellulosic residue. We hypothesize that (1) grapevine cellulosic residue can be solubilized in $ZnCl_2$ solution, crosslinked with Ca^{2+} ions, and plasticized with glycerol to form films, (2) the resulting films will be transparent, and (3) the films will be strong. Herein, grapevine cellulosic residue was extracted, solubilized in $ZnCl_2$ solution, crosslinked with Ca^{2+} ions, and plasticized with glycerol to prepare films. They were characterized for color, transmittance, moisture content, water solubility, water absorption, water vapor permeability, tensile strength, elongation at break, and soil biodegradation. The novelty of this study lies in demonstrating that cellulose extracted from grapevine pruning waste can be used to develop biodegradable films with high transparency and mechanical strength, offering a sustainable and effective alternative for food packaging.

2. Materials and methods

2.1. Materials

The 'Marquette' grapevine canes were collected from the vineyard at South Dakota State University, South Dakota, Brookings, SD, USA. The chemicals potassium hydroxide (Cat# BDH9262-12 KG, Lot# 22H0156406, ≥85%, ACS grade), sodium chlorite (Cat# 127350-10KG, Lot# 50093160, ≥80%, Technical grade), zinc chloride (Cat# 470303-080, Lot# AD-23341, 100%, Lab grade), calcium chloride dihydrate (Cat# BDH9224-1KG, Lot# 22E1056611, ≥99%, ACS grade), glycerol (Cat# BDH1172-19 L, Lot 22H2656009, ≥99.7%, Lab grade), calcium sulfate (Cat# 142305-5LB, Lot# 50104552, ≥98%, ACS grade), and potassium sulfate (Cat# BDH4618-500G, Lot# 23K1056729, ≥99%, ACS grade) were purchased from VWR International, USA. Ethanol (≥99.2%, Lab grade) was obtained from the Department of Chemistry and Biochemistry at South Dakota State University, Brookings, SD.

2.2. Methods

2.2.1. Extraction of cellulosic residue and film preparation. The extraction of cellulosic residue from grapevines and film preparation followed a published protocol.[23] Grapevine canes were dried and ground using a Glen Mills blender (Model: 174937.00, USA) to a 60-mesh size. The pulverized sample underwent two treatment steps: first with 10% (w/v) KOH for 4 hours at 45 °C and 300 rpm, followed by treatment with 10% (w/v) $NaClO_2$ for 10 hours at 70 °C on a hot plate magnetic stirrer at 300 rpm. After each treatment, the residue was thoroughly washed with distilled water until a neutral pH was achieved. The cellulosic residue yield was 28.52%, a value close to those reported in previous studies.[45,46] The obtained cellulosic residue (GVC) was dried at 40 °C for 24 hours in a hot air oven, then milled to a 60-mesh size and stored in an airtight jar for future use.

For film preparation, 0.4 g of GVC was swollen in 1.6 mL of water in a water bath at 63 °C for 2 hours. It was solubilized in a 6 mL 68% $ZnCl_2$ solution for 30 minutes and crosslinked with $CaCl_2$ for 10 minutes.[47] To understand the effect of $CaCl_2$, two

different concentrations, specifically 300 and 400 mM, were used in the filmmaking solution. The total volume of water used was 7.6 mL. To enhance the flexibility of the film, glycerol (10% of GVC) was added to the solution for 5 minutes. The solution was then cast on a 10″ × 12″ glass plate using a handheld applicator while maintaining a 1 mm gap. Subsequently, 500 mL of absolute ethanol was added to the tray with the film-casted glass plate. The mixture was shaken at 50 rpm for 5 minutes using a digital shaker (VWR International, 89032-096, model 3500, USA), after which the film was peeled off, fixed on wood frame, washed with distilled water for 10 minutes to remove excess ethanol and salt, and dried at room temperature (22 ± 2 °C) and relative humidity 47 ± 2% for 24 hours (Fig. 1). Finally, the film was collected and stored in an airtight bag for characterization.

2.2.2. Film characterization. All the film samples were characterized by their spectroscopic properties (transmittance, transparency, absorption coefficient, color, and FTIR), hydration properties (moisture content, water solubility, and water absorption), water vapor permeability, mechanical properties (tensile strength and elongation at break), and soil biodegradability using the established protocols.[39] The optical properties of packaging films, including light transmittance and color, significantly impact consumer perception and visual appeal. Transmittance determines how much light passes through a film, affecting its transparency and the visibility of the packaged product, both of which influence consumers' purchasing decisions. In addition, hydration properties, including water vapor permeability, absorption, and solubility, are critical for understanding a film's interaction with moisture and its ability to preserve product quality and extend shelf life. Mechanical performance, including tensile strength and elongation at break, ensures that the film can withstand stress during handling, transportation, and storage. Similarly,

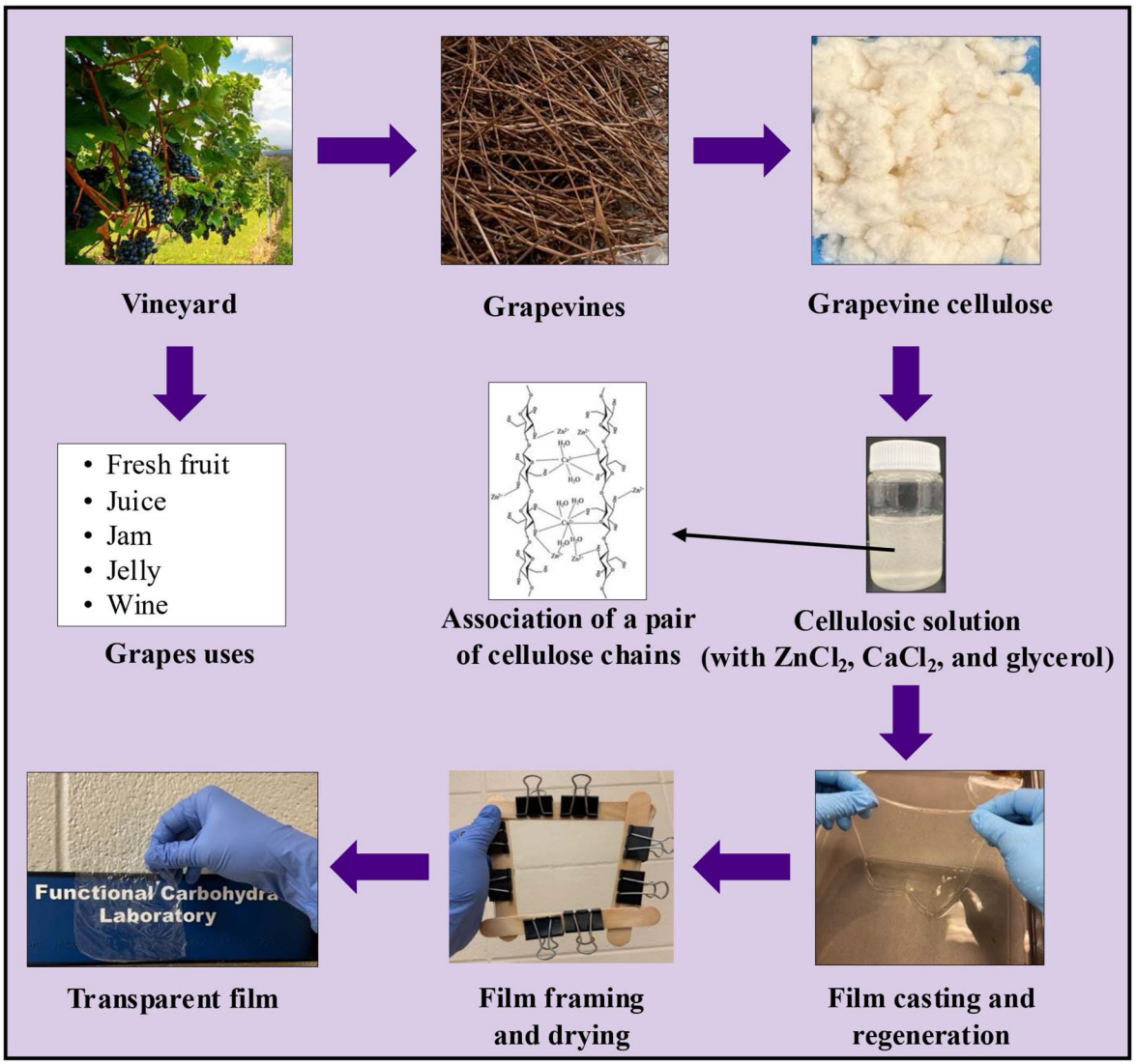

Fig. 1 Cellulosic residue extraction from grapevine canes to develop transparent and biodegradable packaging films. Film color was measured on the Hunter *L*a* b** scale (Nix Pro 2 color sensor, NIXPRO002, Canada). The whiteness index (WI), yellowness index (YI), and total color difference (TCD) were calculated using eqn (3), (4), and (5),[23] respectively.

biodegradation testing assesses the extent to which cellulose films decompose under natural conditions, thereby helping to realize their environmental impact and potential to mitigate landfill and marine pollution. The thicknesses of the 300 and 400 mM $CaCl_2$ films were measured to be 0.04 ± 0.01 and 0.02 ± 0.01 mm, respectively.

The transparency and absorption coefficient of the film were calculated using eqn (1) and (2),[23] respectively. The transmittance was measured using a UV-Vis spectrophotometer (VWR International, Model no: UV-1600PC, 10037-436) at 600 nm. An empty cuvette (Cat# 10037-462, VWR International, USA) with 100% transmittance was used as a blank.

$$\text{Transparency} = \frac{\log(T_{600})}{t} \quad (1)$$

$$\alpha = \frac{1}{t}\ln\left(\frac{1}{T_{600}}\right) \quad (2)$$

wherein, T_{600}: transmittance at 600 nm (%), t: thickness of the film (mm), α: absorption coefficient (mm^{-1}).

$$\text{WI} = 100 - [(100 - L^*)^2 + a^{*2} + b^{*2}]^{0.5} \quad (3)$$

$$\text{YI} = 142.86\frac{b^*}{L^*} \quad (4)$$

$$\text{TCD} = \left[\left(L^* - L_b^*\right)^2 + \left(a^* - a_b^*\right)^2 + \left(b^* - b_b^*\right)^2\right]^{0.5} \quad (5)$$

wherein, L^*, a^*, and b^*: film's color, L_b^*, a_b^*, and b_b^*: background color (for the standard white plate).

FTIR spectra of GVC and films were recorded using the PerkinElmer FTIR Spectrophotometer, Spectrum 100, in the range of 400 to 4000 cm^{-1}, employing 36 scans at a resolution of 4 cm^{-1}. The peak positions of the spectra were examined to analyze the changes that occurred in the film compared to the cellulosic residue.

For moisture content, pre-weighed 3×3 cm films were taken and dried at 105 °C for 24 hours. Then, the final weight was measured, and the moisture content was determined using eqn (6).

$$\text{Moisture (\%)} = \left(\frac{\text{initial weight} - \text{weight after drying}}{\text{initial weight}}\right) \times 100 \quad (6)$$

Films were similarly dried for both water solubility and water absorption tests. The dried film was placed in 100 mL of water in a glass beaker and agitated at 150 rpm for 24 hours using a digital shaker (VWR International, USA). Afterward, it was dried and weighed for the water solubility (WS) test, which was calculated using eqn (7).

$$\text{WS (\%)} = \frac{(\text{initial dried weight} - \text{final dried weight})}{\text{initial dried weight}} \times 100 \quad (7)$$

Likewise, the dried films were soaked in water, and their weight was recorded at 5, 10, 15, 30, 60, and 120 minutes. The water absorption of the film over time was calculated using eqn (8). Furthermore, the water absorption kinetics were analyzed using nine established models, namely Peleg, Peppas, Singh, Gornicki, Pilosof, Czel and Czigany, Vega-Galvez, Garcia-Pascual, and Weibull models, and their respective equations were presented in eqn (9)–(17). The fit of these kinetic models was verified by calculating the coefficient of determination (R^2) and root mean square error (RMSE) using eqn (18) and (19), respectively.

$$\text{Water absorption (\%)} = \frac{\text{water absorped weight} - \text{initial dried weight}}{\text{initial dried weight}} \times 100 \quad (8)$$

$$\frac{t}{m_t} = K_2 t + K_1 \quad (9)$$

$$\frac{\text{mr}_t/\text{mr}_\infty}{t^{1/2}} = K_1 t^{1/2} + K_2 \quad (10)$$

$$\text{mr}_t = a + \frac{b \times t}{c \times t + 1} \quad (11)$$

$$\text{mr}_t = a + b \times \left(1 - \frac{1}{1 + b \times c \times t}\right) \quad (12)$$

$$\text{mr}_t = a + \frac{b \times t}{c + t} \quad (13)$$

$$\text{mr}_t = a \times t^{\text{m}} \quad (14)$$

$$\text{mr}_t = a \times \exp\left[-\frac{b}{(1+t)^{\alpha}}\right] \quad (15)$$

$$\text{mr}_t = 1 - \exp\left[\left(-\frac{t}{a}\right)^b\right] \quad (16)$$

$$\text{mr}_t = m_e \times (m_o - m_e)\exp(-t/\beta)^{\alpha} \quad (17)$$

$$R^2 = 1 - \frac{\sum (y_i - \hat{y})^2}{\sum (y_i - \bar{y})^2} \quad (18)$$

$$\text{RMSE} = \sqrt{\frac{\sum (y_i - \hat{y})^2}{N}} \quad (19)$$

Herein, t: time (in min), m_t: moisture content (%) at time 't'. mr_t: moisture ratio at time 't'. mr_∞ and m_e: moisture ratio at 120 min. m: Czel and Czigany model's slope of the curve fitting. K_1 and K_2: intercept and slope of curve fitting in the Peleg model, respectively. K_2 and K_1: Intercept and slope of curve fitting in the Peppas model, respectively. a, b, c, α, and β: constants ($\alpha = 0.9$, a fixed value for Vega-Galvez's model only).

For water vapor permeability (WVP), the desiccator's relative humidity (RH) was maintained at approximately 97% using a saturated K_2SO_4 solution. Later, a film-sealed glass vial was maintained at approximately 0% relative humidity (RH) with 4 g of anhydrous $CaSO_4$. The initial weight of the vial was recorded and measured every hour for eight hours. The rate of weight change was calculated per unit of time and surface area of the

film to determine the water vapor transmission rate (WVTR) using eqn (20). The WVP was then calculated using eqn (21).[24]

$$\text{WVTR}\ \left(\text{g m}^{-2}\ \text{s}^{-1}\right) = \frac{(\Delta W/\Delta t)}{A} \tag{20}$$

$$\text{WVP} = \frac{\text{WVTR}}{P(R_1 - R_2)} \times t \tag{21}$$

wherein, $\Delta W/\Delta t$: rate of weight gain (g s^{-1}), obtained from the slope of the weight *vs.* time plot. A: surface area of film used in covering the vial's orifice. P: saturation vapor pressure of water (Pa) at 25 °C. R_1: RH in the desiccator. R_2: RH in the cup. t: film thickness (m) measured with a Vernier caliper (RexBeti, China). The driving force $[P(R_1 - R_2)]$ in the experimental condition was calculated as 3073.93 Pa.

The tensile strength (TS) and elongation at break (EB) were measured using the Texture Analyzer (Stable Micro Systems, Model TA-HD plus, serial no: 5529). Eqn (22) and (23) were used for calculation, respectively. Here, a film strip 1 × 8 cm long was fitted in the grip, with a 6 cm gap. A trigger force of 50 N and an elongation speed of 15 mm s^{-1} were used.

$$\text{TS (MPa)} = \frac{\text{force used to break film (N)}}{\text{film's surface area (mm}^2\text{)}} \tag{22}$$

$$\text{EB (\%)} = \frac{\text{change in length (mm)}}{\text{initial length (mm)}} \times 100 \tag{23}$$

For the soil biodegradability test, the soil's moisture content was maintained at 24 ± 2% throughout the process by applying the Pearson square method calculation. A pre-weighed film strip measuring 3 × 3 cm, was embedded in the soil, and the weight was taken every 2 days. Eqn (24) was used to calculate % biodegradation,[48] and their first-order and second-order reaction reduction kinetics were determined using eqn (25) and (26), respectively. The R^2 and RMSE values were calculated using eqn (18) and (19), respectively. The half-life was calculated using the best-fitting model.

$$\%\ \text{Biodegradation} = \frac{\text{loss in film weight} \times 100}{\text{initial weight}} \tag{24}$$

$$\ln(y) = mx + c \tag{25}$$

$$\ln(y) = a + bx + cx^2 \tag{26}$$

wherein, ln(y): natural logarithm of % biodegradation. x: biodegradation days. m and c: slope and intercept, respectively, in eqn (25). a, b, and c: constants in eqn (26).

2.2.3. Statistical analysis. The average value and standard deviation were reported from the triplicate measurements using three independent batches during the study. A Welch two-sample t-test was performed using RStudio (Version 2024.09.1+394) to determine if the data significantly differed at a 5% level of significance. The water absorption and soil biodegradation kinetics were calculated using Microsoft Excel for Mac (Version 16.88 (24081116)) with Solver add-ins.

3. Results and discussion

3.1. Spectroscopic properties

3.1.1. Transparency and transmittance of electromagnetic radiation. The transparency of GVC films increases with a higher concentration of $CaCl_2$, rising from 83.7 ± 0.1% mm^{-1} at 300 mM to 84.3 ± 0.2% mm^{-1} at 400 mM $CaCl_2$. However, this difference is not statistically significant ($p > 0.05$). These values closely align with those of films made from wood cellulose at 86.2%,[49] durian-rind cellulose at 86%,[50] wood cellulose nanopaper at 90%,[51] and low-density polyethylene at 80%,[52] and some of which are listed in Table 1. Transmittance levels exceeding 80% result in a transparent film, a feature that consumers value highly as it allows them to assess the quality of food products before purchase. Therefore, GVC films are an excellent choice for packaging applications.

The absorption coefficient was 7.6 ± 0.3 for GV300 films and 6.1 ± 0.4 for GV400 films. A study reported an absorption coefficient ranging from 0.4 to 9.1 in cellulose and lignin-blend films.[53]

3.1.2. Color. The color profile of GVC films was assessed using Hunter's scale, with L, a, and b values indicating lightness, red-green, and yellow-blue, respectively. GV300 exhibited L, a, and b values of 83.95 ± 0.11, 2.90 ± 0.09, and 0.74 ± 0.20. In contrast, GV400 displayed significantly higher L and lower a value of 85.90 ± 0.01 and 0.08 ± 0.05 ($p < 0.05$), respectively, with a b value of 0.55 ± 0.03. These findings indicate an increase in the lightness of the film with the addition of Ca^{2+} ions. GV300 recorded TCD, WI, and YI values of 24.73 ± 0.70, 83.67 ± 0.11, and 1.26 ± 0.34, whereas GV400 showed values of 5.11 ± 0.02, 85.89 ± 0.01, and 0.92 ± 0.05, respectively. These values are comparable to those of cellulose-based films (Table 1).

3.1.3. FTIR. The major FTIR spectral peaks of GVC were observed at 895, 1027, 1048, 1081, 1159, 1316, 1368, 1428, 1610, 2893, 3295, and 3332 cm^{-1} (Fig. 2a). In this set, the 895 and 1316 cm^{-1} bands were retained in the film, while the 1048, 1081, and 3295 cm^{-1} peaks disappeared. The remaining peaks shifted as follows: 1027 to 1017 and 1018, 1159 to 1157 and 1156, 1368 to 1372 and 1372, 1428 to 1417 and 1416, 1610 to 1615 and 1615, 2893 to 2894 and 2902, and 3332 to 3326 and 3331 cm^{-1} for the GV300 and GV400 films, respectively, as shown in Fig. 2b and c. Additionally, two peaks at 995 and 2920 cm^{-1} were also observed in the films. The disappearance, shifting, and new formation of peaks resulted from interactions among cellulosic residue, zinc ions, calcium ions, and glycerol molecules in the film.

The peak at 895 cm^{-1} indicates the β-glycosidic linkage in cellulose.[59–61] The bands at 1027 and 1081 cm^{-1} correspond to the C–O–C linkage in the cellulosic residue,[62] the shifting of the 1027 cm^{-1} peak in the films could be due the change in crystallinity and polymer chain packing, and the disappearance of the 1081 cm^{-1} peak suggests a weakening of the linkage in the film due to cellulose dissolution. The peak at 1048 cm^{-1} results from C3···O3H bond vibration, and its absence in the film implies the formation of O3H···Zn interactions in the cellulosic chains during solubilization.[47] The bands at 1159, 1316, and

Table 1 Comparison of grapevine cellulose films' color in Hunter scale (*L*, *a*, *b*, total color difference (TCD), yellowness index (YI), and whiteness index (WI)) and transparency (Trans, % mm^{-1}), with some biopolymer films

Sample	*L*	*a*	*b*	TCD	YI	WI	Trans	Reference
GV300	83.95 ± 0.11	2.90 ± 0.09	0.74 ± 0.20	24.73 ± 0.70	1.26 ± 0.34	83.67 ± 0.11	84.00 ± 0.57	This study
GV400	85.90 ± 0.01	0.08 ± 0.05	0.55 ± 0.03	5.11 ± 0.02	0.92 ± 0.05	85.89 ± 0.01	86.85 ± 0.78	This study
Alfalfa cellulose	87.3	0.7	6.6	85.6	10.8	6.8	27.3	23
Avocado peel fiber	82.8–85.2	1.4–2.7	4.1–7.2	5.9–9.1	81.6–84.6	—	86.7–89.2	25
Banana peel fiber	81.7–84.7	0.7–1.0	3.9–5.3	3.5–6.2	6.5–9.2	80.9–84.2	32.0–45.1	26
Carboxymethyl cellulose/hemicellulose/methylcellulose	84.7–88.0	1.2–3.0	11.7–18.4	15.0–132.9	19.0–31.0	75.9–83.2	—	54
Cellulose	78.6–86.4	−2.1–2.4	−2.4–2.0	1.6–9.5	−4.3–2.3	78.5–86.4	10.5–18.9	55
Kodo millet starch	23.9–86.9	−0.6–3.6	2.0–11.5	11.1–70.5	—	—	1.0–16.2	56
Palm sprout peel	14.9–24.1	−0.2–0.2	−2.2–0.02	1.8–3.8	—	—	77.6–92.4	57
Sodium caseinate/halloysite nanoclay	87.3–89.7	−2.2–3.0	5.1–8.0	7.6–10.9	—	—	—	58
Corncob cellulose	83.2	1.7	6.9	8.7	11.9	81.7	28.6	37
Soyhull cellulose	85.1	0.6	4.3	5.3	7.2	84.5	30.9	24
Soyhull lignocellulose	77.2	4.7	10.7	17.3	19.9	74.4	37.6	39
Soyhull lignocellulose extract	79.9	3.8	12.2	15.9	21.9	76.1	31.5	38
Spent coffee grounds lignocellulose	31.3–45.6	0.8–1.3	7.3–15.5	41–61	30–45	24–75	13–19.5	40
Switchgrass lignocellulose	88.0–89.3	0.3–0.5	3.5–3.6	2.8–3.4	5.6–5.9	87.5–88.7	13.1–16.7	42
Switchgrass lignocellulosic extract	73.6–76.4	1.2–1.7	17.7–30.8	23.6–33.0	34.4–57.6	61.1–68.2	9–15	41
Wheat straw fiber	88.2–88.7	0.5–0.8	1.7–2.5	2.6–3.1	2.8–4.0	—	5.3–6.6	43

1368 cm^{-1} signify the asymmetric C–O–C stretching vibration of the glycosidic linkage, CH_2 bending, and the presence of xyloglucan, respectively.[63] The peak at 3295 cm^{-1} is attributed to the stretching vibration of OH groups,[64] which weakens during the filmmaking process and diminishes completely. Similarly, the peak at 1428 cm^{-1} indicates the presence of the xylan group exhibiting CH_2 vibrations and the shifting might be due to changes in the hydrogen bonding interactions in the film matrix, while peaks at 1610, 2892, and 3332 cm^{-1} represent the mannan group with CO, CH_2, and OH vibrations, respectively, in the cellulosic residue. Their shifting is due to a subtle change in hydrogen bonding interactions between mannan and cellulose chains in the cellulosic residue.[24,37,65–67] The new peaks at 995 and 2920 cm^{-1} in the film are more likely due to the formation of new C–O and C–H stretching, respectively. Overall, the FTIR spectrum reveals the coexistence of xylan and mannan groups alongside cellulose in the cellulosic residue.

3.2. Hydration properties

3.2.1. Moisture content. Film properties such as moisture content, water solubility, water absorption, and water vapor permeability are essential parameters to study, as they influence the mechanical, barrier, and biodegradation properties of films. The moisture content was 11.78 ± 0.24% for GV300 and 10.37 ± 0.39% for GV400, indicating a decrease with higher calcium chloride content. However, this difference was not statistically significant (p-value > 0.05). A similar trend was observed with banana peel fiber, where the addition of Ca^{2+} ions reduced the water-holding capacity of the films.[26] The moisture content is comparable to that of ambarella fruit peel and jackfruit seed slimy sheath pectin films, which have moisture contents ranging from 9.35% to 10.87%.[68] A few comparable films are listed in Table 2.

3.2.2. Water solubility. The water resistance of packaging materials is crucial for maintaining product shelf life by preventing moisture transfer that can lead to deterioration.[77] Therefore, investigating the water solubility (WS) of biodegradable films is essential for understanding their moisture sensitivity. Films with low WS can better withstand humid conditions, making them ideal for food packaging. The WS of the films was 18.60 ± 0.33% and 13.91 ± 0.17% for calcium chloride concentrations of 300 mM and 400 mM, respectively. WS significantly decreased as the calcium chloride concentration increased from 300 mM to 400 mM (p-value = 0.0104). A similar trend of decreasing WS with increased crosslinking by Ca^{2+} ions has been reported in films made from avocado peel fiber,[25] switchgrass lignocellulose,[42] banana peel fibers,[26] and wheat straw lignocellulosic fibers,[43] all of which show comparable water solubility (Table 2).

3.2.3. Water absorption and kinetics. To further understand water affinity, the water absorption of films was studied over time. Water absorption in biodegradable films is crucial for analyzing their interaction with moisture, influencing their structural integrity and flexibility.[78] Controlled water absorption helps maintain the film's strength in humid conditions. The water absorption of GV400 was 163.59 ± 6.08% at 5 minutes,

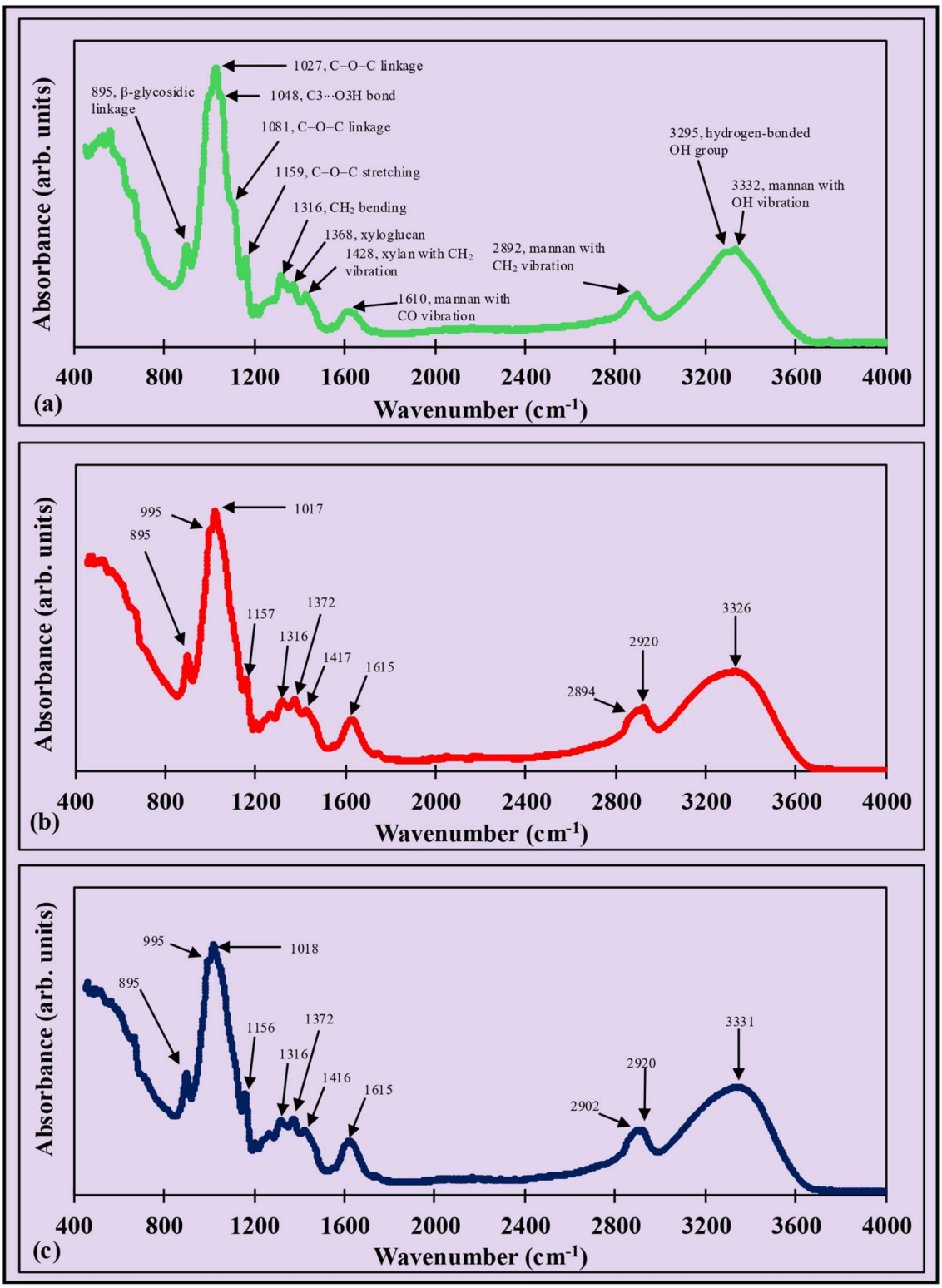

Fig. 2 FTIR peaks of (a) grapevine cellulose, (b) GV300 film, and (c) GV400 film. The functional group identified for grapevine cellulose also corresponds to the peaks of the films.

gradually increasing to 168.30 ± 8.70%, 171.19 ± 9.78%, 177.69 ± 8.85%, 180.93 ± 8.39%, and 184.51 ± 4.36% at 10, 15, 30, 60, and 90 minutes, respectively, ultimately reaching 191.35 ± 1.91% at 120 minutes (Fig. 3a). In contrast, GV300 showed a higher water absorption of 196.17 ± 0.36%, 208.33 ± 1.68%, 231.46 ± 2.65%, 237.50 ± 2.53%, 241.24 ± 0.60%, 245.59 ± 0.48%, and 254.00 ± 2.77% at 5, 10, 15, 30, 60, 90, and 120 minutes, respectively. The rise in the Ca^{2+} ions enhances the

Table 2 Comparison of the moisture content (MC), solubility (Sol), water absorption at 120 minutes (WA_{120}), water vapor permeability (WVP), tensile strength (TS), elongation at break (EB), 90% film biodegradation at 24% soil moisture (Bio_{90}), and half-life of film biodegradation (HL) of grapevine cellulose films compared to some biopolymer films

Sample	MC (%)	Sol (%)	WA_{120} (%)	WVP (10^{-10} g m^{-1} s^{-1} Pa^{-1})	TS (MPa)	EB (%)	Bio_{90} (days)	HL (days)	Reference
GV300	11.78 ± 0.24	18.60 ± 0.33	254.0 ± 2.8	1.42 ± 0.11	15.42 ± 0.54	8.61 ± 0.39	15	8.5	This study
GV400	10.37 ± 0.39	13.91 ± 0.17	191.4 ± 1.9	0.74 ± 0.10	18.20 ± 0.71	6.07 ± 0.44	17	9.0	This study
Alfalfa cellulose	10.0	9.2	152.0	0.47	16.9	10.1	35	25.8	23
Avocado peel fiber	14.2–20.8	15.7–21.8	30–52	2.4–2.5	7.2–15.7	5.2–13.6	28	3.2–4.6	25
Banana peel fiber	13.7–22.3	24.5–65.7	98.0–156.0	2.4–3.6 × 10^3	16.3–31.3	4.9–13.0	30	15.3–20.7	26
Carboxymethyl cellulose	—	—	—	48.6–214.0	2.1–22.0	6.7–45.1	—	—	69
Carboxymethyl cellulose/hemicellulose/methylcellulose	8–13	—	—	0.8–2.4 × 10^5	5.0–10.5	105.0–137.2	—	—	54
Carboxymethyl starch/PVA	—	—	—	1.3–1.6	35.1–42.9	35.6–75.3	—	—	70
Cattail flower cellulose	3.1–4.5	2.0–22.3	—	—	—	—	—	—	71
Cellulose	6.5–13.8	12.5–52.6	17.2–149.0	0.6–12.2	0.3–22.4	4.3–13.2	33–60	20.6–53.3	55
Cellulose acetate		1.5–15.4		47.2–233.3	0.1–3.2	0.2–9.5			72
Corn bran arabinoxylan	14.8–17.0	79.9–96.9	—	—	—	—	—	—	73
Corncob cellulose	10.1	64.1	15.7	1.8	4.7	15.4	29	13.9	37
Jamun seed starch	16.4–19.2	16.5–30.5	—	—	5.0–20.0	25.0–60.9	—	20	74
Kodo millet starch	14.4–16.5	31.1–37.7	—	—	9.3–13.2	2.0–8.0	—	—	56
Nacre-like carboxymethyl cellulose	13.6–20.5	6.3–90.0	—	—	29.0–63.6	40.0–80.0	—	—	75
Palm sprout peel	0.2–20.7	0.0–92.0	—	0.1–9.2 × 10^5	4.0–11.2	4.8–80.4	—	15	57
Sodium caseinate/halloysite nanoclay	7.9–13.5	9.5–20.6	—	—	3.8–4.9	71.0–120.0	—	—	58
Soyhull cellulose	8.4	69.6	82.1	0.9	6.3	30.2	25	11.6	24
Soyhull lignocellulose	12.9	26.0	37.7	0.3	9.3	8.8	37	21.6	39
Soyhull lignocellulose extract	11.2	7.6	118.9	0.2	16.8	14.7	33	20.1	38
Spent coffee grounds lignocellulose	6–8	—	19.5–79.3	0.8–1.8	8.4–26.8	3.8–7.9	45	14.7–20.1	40
Switchgrass lignocellulose	11.3–14.1	58.7–71.2	275.0–293.8	0.1–0.2	9.9–14.7	3.4–4.7	35	16.2–19.3	42
Switchgrass lignocellulosic extract	12.5–17.8	48.3–68.2	209.5–220	0.2–0.3	8.9–12.7	2.2–2.4	35	15–17	41
Walnut/mango/orange peel	8.4–36.3	7.8–39.8	—	—	—	—	—	—	76
Wheat straw fiber	14.4–24.3	28.7–56.9	12.3–56.1	1.9–2.4	5.3–6.6	16.4–27.3	28	2.0–5.0	43

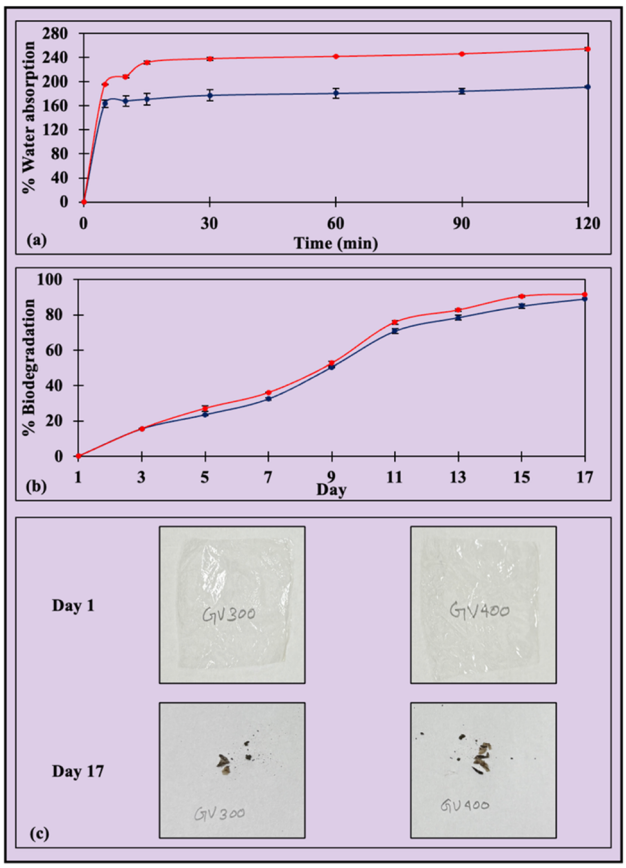

Fig. 3 Trends in (a) water absorption and (b) biodegradation of grapevine cellulose films. The red and blue lines represent samples GV300 and GV400, respectively. (c) The films lose weight and size from day 1 to day 17 during the biodegradation process.

structural integrity of the film, thereby resulting in a reduction in hydrophilicity due to denser network formation and a decrease in water absorption in GV400.[24] The highest water absorption values of several known films are listed in Table 2. The analysis of the water absorption behavior of the films (Table S1†) suggests that the Peleg model kinetics are the best-fitting option for both GV300 and GV400, with the highest R^2 values of 0.9994 and 0.9992 and the lowest RMSE values of 0.0039 and 0.0061, respectively, compared to other models. In the Peleg model, the lower K_1 and K_2 values indicate the initial higher water absorption and a greater water absorption capacity of the film, respectively. Here, the GV300 film had lower K_1 and K_2 values than the GV400 film and demonstrated lower water absorption, further signifying the fitting of the Peleg model. Films composed of cellulose,[55] soyhull cellulose,[24] corncob cellulose,[37] avocado peel fiber,[25] soyhull lignocellulose,[39] agar,[79] spent coffee grounds lignocellulose,[40] and alfalfa cellulose[23] also conformed to the Peleg model.

3.2.4. Water vapor permeability. The water barrier properties of films were assessed by calculating water vapor permeability (WVP); lower WVP values indicate superior water barrier performance. Measuring WVP is essential for understanding how effectively a packaging film can control moisture transfer. It determines the film's ability to protect food products from drying out or becoming overly moist, which directly affects their shelf life and quality. WVP is crucial for selecting suitable films for various food and storage environments.[80–82] The WVP of GVC films decreased with increased $CaCl_2$ concentration, measuring $1.42 \pm 0.11 \times 10^{-10}$ g m^{-1} s^{-1} Pa^{-1} at 300 mM. It significantly dropped (p-value 0.0231) to $0.74 \pm 0.10 \times 10^{-10}$ g m^{-1} s^{-1} Pa^{-1} at 400 mM $CaCl_2$. The increased crosslinking of cellulose chains with higher amounts of calcium ions results in a compact network structure with reduced free space within the film matrix, leading to a lower WVP. Similar values of 2.95–4.70, 0.6–12.15, 0.7–1.9, and $1.7–2.3 \times 10^{-10}$ g m^{-1} s^{-1} Pa^{-1} have been reported for dragon fruit peel pectin/potato starch films,[83] cellulose films,[55] alginate-collagen films,[84] soyhull cellulose films,[24] and corncob cellulose films,[37] respectively (Table 2).

3.3. Tensile strength and elongation at break

GVC films were tested for tensile strength (TS) and elongation at break (EB) to evaluate their strength and flexibility, the primary parameters for packaging materials that support the product. The TS of GV300 was 15.42 ± 0.54 MPa, increasing to 18.20 ± 0.71 MPa in GV400 with higher concentrations of Ca^{2+} ions. During film preparation, when cellulosic residue is added to the zinc chloride solution, O3H···Zn interactions occur, as shown by the disappearance of the 1048 cm^{-1} peak in the FTIR. Consequently, the intra-chain O3···O5H bonds that provide rigidity to the cellulosic residue are broken, resulting in pliable chains that allow water penetration in the cellulosic network and, in turn, solubilize the cellulosic residue. The subsequent addition of calcium ions crosslinks the non-rigid Zn-cellulosic residue chains, increases solution viscosity, and leads to stronger films.[47] As more calcium ions are incorporated, increased crosslinking results in higher tensile strengths of the films, as observed with GV400 compared to GV300. A similar trend of increasing TS with higher concentrations of Ca^{2+} ions has also been noted in cellulose films,[55] corncob cellulose films,[37] soyhull cellulose,[24] soy hull lignocellulose,[39] and alfalfa cellulose films.[23] These values are comparable to those of other films (Table 2), such as carrageenan/cassava starch, avocado peel fiber, chitin, cellulose nanofiber, and wheat straw fibers, which exhibit strengths of 6.53–25.88 MPa,[85] 7.15–15.74 MPa,[25] 4.7–16.2 MPa,[86] 7.6–15.2 MPa,[87] and 6.61 MPa,[43] respectively. However, the TS of GVC films is lower than that of PLA films of 55.6 MPa,[88] and higher than starch films of 5.21 MPa.[89]

The EB of GVC films was $8.61 \pm 0.39\%$ at a 300 mM $CaCl_2$ concentration, decreasing to $6.07 \pm 0.44\%$ at a 400 mM $CaCl_2$ concentration. The presence of Ca^{2+} ions significantly ($p < 0.05$) lowered the EB of the films. Nevertheless, glycerol has been utilized as a plasticizer, recognized for its ability to enhance EB.[55,72,90,91] This trend corresponds with banana peel fiber films, where the EB decreases from 12.97% to 4.85% as the $CaCl_2$ concentration increases from 200 to 500 mM. The increase in $CaCl_2$ concentration increases strength but reduces flexibility. The higher strength, low-flexibility films can be helpful for rigid packaging, while high flexibility can be used for packaging soft and irregularly shaped products. Thus, $CaCl_2$ concentration is

crucial for specific packaging applications. The elongation property of GVC films closely relates to those of other biodegradable films (Table 2), such as pectin (4.53–24.16%),[92] pumpkin-based protein/pectin (13.13–14.37%),[93] fish gelatin/orange peel (4.36–10.97%),[94] carboxymethyl cellulose (7.3–7.7%),[95] PLA (16.4%),[88] and starch (61.7%).[89] However, the EB of biopolymer films is generally much lower than that of commercial plastics; for instance, low-density polyethylene film shows an EB of 300–900%.[96]

3.4. Soil biodegradation

Approximately 90% of GVC films biodegrade in soil with a moisture content of 24% within 17 days (Fig. 3c). The weight reduction and visual observation were used to assess degradation both quantitatively and qualitatively. A weight reduction of 15.7 ± 0.1% was recorded on the third day, which gradually increased to 27.1 ± 1.5%, 36.0 ± 0.2%, 52.6 ± 1.3%, 75.8 ± 1.1%, 82.7 ± 0.9%, 90.5 ± 0.4%, and 91.6 ± 0.3% on the 5th, 7th, 9th, 11th, 13th, 15th, and 17th day, respectively, for the GV300 film (Fig. 3b). In contrast, the weight reduction for the GV400 film was slightly lower, measuring 15.5 ± 0.1% on the third day, which further increased to 23.5 ± 0.1%, 32.5 ± 0.7%, 50.5 ± 0.1%, 70.8 ± 1.5%, 79.0 ± 1.3%, 85.0 ± 1.4%, and 89.1 ± 0.6%. Ca^{2+} ions that form strong crosslinks between Zn-cellulosic chains, creating a dense network structure, may hinder microbial activity, thereby indicating that increased $CaCl_2$ concentration in GV400 could slow down the biodegradation process.[24] Similarly, about 90% of the wheat straw fiber films biodegraded on the 28th day,[43] spent coffee ground films on the 45th day,[40] and cellulose films on the 29th day.[37] Furthermore, the biodegradation behavior of GVC films was studied using first and second-order reaction kinetics (Table S1†). Higher R^2 and lower RMSE values were used to identify the best-fitting reaction model. The R^2 and RMSE values for the first-order reaction kinetics of GV300 and GV400 films were 0.9032 and 0.1897, and 0.9171 and 0.1777, respectively. Conversely, the values for GV300 in second-order reaction kinetics were 0.9945 and 0.0451, while for GV400, they were 0.9931 and 0.0514. The best-fitting model was determined to be second-order kinetics, which was further utilized to calculate the biodegradation half-life of GVC films.

The half-life was 8.5 and 9.0 days for GV300 and GV400 films, respectively. The half-life of several biopolymer films ranges from 20.6 to 53.3 days,[55] 13.9 days,[37] 16.2 to 19.1 days,[42] 3.2 to 4.6 days,[25] 15 to 17 days,[41] 2 to 5 days,[43] 15.3 to 20.7 days,[26] 11.6 days,[24] and 1.2 to 7.2 days[97] for cellulose, corncob cellulosic residue, switchgrass lignocellulosic residue, avocado peel fiber, alkali-digested switchgrass lignocellulose, wheat straw biomass, banana peel fiber, soyhulls cellulosic residue, and starch films, respectively (Table 2). The biodegradation half-life is dependent on the film composition, soil moisture content, and soil microbial load, and further research is necessary to understand the influence of these parameters.

4. Conclusions

The widespread use of petroleum-based plastic packaging drives the search for biodegradable alternatives, primarily sourced from agricultural biowaste. This study reports on the utilization of cellulosic residue from underutilized grapevine prunings to create eco-friendly packaging films. The films were formed by solubilizing grapevine cellulose in a $ZnCl_2$ solution, crosslinked with calcium ions, and plasticized with glycerol, validating the first research hypothesis. The physical, mechanical, optical, and biodegradation properties were examined. Notably, GVC films are highly transparent, achieving 83.7–84.3% mm^{-1} transparency, further confirming the second research hypothesis. This high transmittance in packaging films enhances product visibility, making them more attractive to consumers and facilitating easy quality inspection without the need for unsealing. The films biodegrade in soil with a 24% moisture content within 17 days, leaving no lasting environmental impact. The films exhibit high tensile strength (TS) of 15.4–18.2 MPa, supporting the third research hypothesis. The high TS of the GVC film signifies its ability to withstand strong pulling or stretching forces without deforming, tearing, or breaking. This property enhances the film's suitability for handling and transportation of food products by reducing the risk of damage during use. While these attributes highlight the strong potential of GVC films for food packaging applications, it is essential to conduct comprehensive toxicity assessments to ensure food safety. Additionally, the utilization of lignin and hemicellulose fractions from grapevines will significantly contribute to the circular bioeconomy, directing our future research. Overall, using underutilized grapevine prunings as a cellulose source for packaging films enhances waste management in the field and addresses the global issue of plastic pollution. Therefore, developing eco-friendly films from grapevine cellulose represents a practical approach to sustainability, helping to conserve the environment and its resources.

Data availability

Data will be made available on request.

Author contributions

Sandeep Paudel: data curation; formal analysis; methodology; investigation; visualization; software; validation; writing—original draft; review & editing. Sumi Regmi: data curation; formal analysis; methodology; investigation; visualization; writing—original draft; review & editing. Sajal Bhattarai: methodology; investigation; software; validation. Anne Fennell: conceptualization; writing—review & editing. Srinivas Janaswamy: conceptualization; methodology; resources; writing—review & editing; supervision; project administration; funding acquisition.

Conflicts of interest

There are no conflicts to declare.

Acknowledgements

This research was partially funded by the USDA National Institute of Food and Agriculture, SD00G677-20, 2021-67022-33469,

SD00H772-22, and SD00H765-22, and the National Science Foundation (NSF), 1546859. We thank Dr Kasiviswanathan Muthukumarappan for access to the Texture Analyzer and Dr Todd Letcher for access to FTIR.

References

1 M. Kedzierski, D. Frère, G. Le Maguer and S. Bruzaud, Why is there plastic packaging in the natural environment? Understanding the roots of our individual plastic waste management behaviours, *Sci. Total Environ.*, 2020, **740**, 139985.
2 P. M. Coelho, B. Corona, R. ten Klooster and E. Worrell, Sustainability of reusable packaging–Current situation and trends, *Resour., Conserv. Recycl.*, 2020, **6**, 100037.
3 R. Geyer, J. R. Jambeck and K. L. Law, Production, use, and fate of all plastics ever made, *Sci. Adv.*, 2017, **3**, 3–8.
4 D. Cudjoe and H. Wang, Plasma gasification *versus* incineration of plastic waste: Energy, economic and environmental analysis, *Fuel Process. Technol.*, 2022, **237**, 107470.
5 C. M. Waluda and I. J. Staniland, Entanglement of Antarctic fur seals at Bird Island, South Georgia, *Mar. Pollut. Bull.*, 2013, **74**, 244–252.
6 S. Dey, G. T. N. Veerendra, P. S. S. A. Babu, A. V. P. Manoj and K. Nagarjuna, Degradation of plastics waste and its effects on biological ecosystems: A scientific analysis and comprehensive review, *Biomed. Mater. & Devices*, 2024, **2**, 70–112.
7 C. Thiagarajan and Y. Devarajan, The urgent challenge of ocean pollution: Impacts on marine biodiversity and human health, *Reg. Stud. Mar. Sci.*, 2025, **81**, 103995.
8 T. A. Kurniawan, A. Mohyuddin, M. H. D. Othman, H. H. Goh, D. Zhang, A. Anouzla, F. Aziz, J. C. Casila, I. Ali and B. Pasaribu, Beyond surface: Unveiling ecological and economic ramifications of microplastic pollution in the oceans, *Water Environ. Res.*, 2024, **96**, e11070.
9 M. R. Shekh and V. Kumar, Impact of plastic pollution on ecosystems: A review of adverse effects and sustainable solutions, *Environ. Monit. Assess.*, 2025, **197**, 264.
10 J. C. Prata, J. P. da Costa, I. Lopes, A. C. Duarte and T. Rocha-Santos, Environmental exposure to microplastics: An overview on possible human health effects, *Sci. Total Environ.*, 2020, **702**, 134455.
11 G. Kutralam-Muniasamy, V. C. Shruti, F. Pérez-Guevara and P. D. Roy, Microplastic diagnostics in humans: "The 3Ps" Progress, problems, and prospects, *Sci. Total Environ.*, 2023, **856**, 159164.
12 K. D. Cox, G. A. Covernton, H. L. Davies, J. F. Dower, F. Juanes and S. E. Dudas, Human consumption of microplastics, *Environ. Sci. Technol.*, 2019, **53**, 7068–7074.
13 Y. Lee, J. Cho, J. Sohn and C. Kim, Health effects of microplastic exposures: Current issues and perspectives in South Korea, *Yonsei Med. J.*, 2023, **64**, 301–308.
14 A. Thulasisingh, K. Kumar, B. Yamunadevi, N. Poojitha, S. SuhailMadharHanif and S. Kannaiyan, Biodegradable packaging materials, *Polym. Bull.*, 2022, **79**, 4467–4496.
15 Q. Xia, C. Chen, Y. Yao, J. Li, S. He, Y. Zhou, T. Li, X. Pan, Y. Yao and L. Hu, A strong, biodegradable and recyclable lignocellulosic bioplastic, *Nat. Sustain.*, 2021, **4**, 627–635.
16 I. D. Ibrahim, Y. Hamam, E. R. Sadiku, J. M. Ndambuki, W. K. Kupolati, T. Jamiru, A. A. Eze and J. Snyman, Need for sustainable packaging: An overview, *Polymers*, 2022, **14**, 1–16.
17 D. Klemm, B. Heublein, H.-P. Fink and A. Bohn, Cellulose: Fascinating biopolymer and sustainable raw material, *Angew. Chem., Int. Ed.*, 2005, **44**, 3358–3393.
18 S. Janaswamy, M. P. Yadav, M. Hoque, S. Bhattarai and S. Ahmed, Cellulosic fraction from agricultural biomass as a viable alternative for plastics and plastic products, *Ind. Crops Prod.*, 2022, **179**, 114692.
19 S. Hussain, R. Akhter and S. S. Maktedar, Advancements in sustainable food packaging: From eco-friendly materials to innovative technologies, *Sustainable Food Technol.*, 2024, **2**, 1297–1364.
20 A. S. Khandeparkar, R. Paul, A. Sridhar, V. V. Lakshmaiah and P. Nagella, Eco-friendly innovations in food packaging: A sustainable revolution, *Sustainable Chem. Pharm.*, 2024, **39**, 101579.
21 M. J. Ahmed, J. Ashfaq, Z. Sohail, I. A. Channa, A. Sánchez-Ferrer, S. N. Ali and A. D. Chandio, Lignocellulosic bioplastics in sustainable packaging – Recent developments in materials design and processing: A comprehensive review, *Sustainable Mater. Technol.*, 2024, **41**, e01077.
22 B. K. Dejene and T. M. Geletaw, Development of fully green composites utilizing thermoplastic starch and cellulosic fibers from agro-waste: A critical review, *Polym.-Plast. Technol. Mater.*, 2024, **63**, 540–569.
23 S. Paudel and S. Janaswamy, Use of alfalfa cellulose for formulation of strong, biodegradable film to extend the shelf life of strawberries, *Int. J. Biol. Macromol.*, 2025, **290**, 139004.
24 S. Regmi and S. Janaswamy, Biodegradable films from soyhull cellulosic residue with UV protection and antioxidant properties improve the shelf-life of post-harvested raspberries, *Food Chem.*, 2024, **460**, 140672.
25 S. Ahmed and S. Janaswamy, Strong and biodegradable films from avocado peel fiber, *Ind. Crops Prod.*, 2023, **201**, 116926.
26 M. Hoque and S. Janaswamy, Biodegradable packaging films from banana peel fiber, *Sustainable Chem. Pharm.*, 2024, **37**, 101400.
27 H. Gupta, H. Kumar, M. Kumar, A. K. Gehlaut, A. Gaur, S. Sachan and J.-W. Park, Synthesis of biodegradable films obtained from rice husk and sugarcane bagasse to be used as food packaging material, *Environ. Eng. Res.*, 2019, **25**, 506–514.
28 P. N. Villa, *Global Production of Fruit by Variety Selected 2023*, **https://www.statista.com**, accessed 30 March 2025.
29 A. C. Kılınc, M. Atagur, O. Ozdemir, I. Sen, N. Kucukdogan, K. Sever, O. Seydibeyoglu, M. Sarikanat and Y. Seki, Manufacturing and characterization of vine stem reinforced high density polyethylene composites, *Composites, Part B*, 2016, **91**, 267–274.

30 L. Senila, I. Tenu, P. Carlescu, O. R. Corduneanu, E. P. Dumitrachi, E. Kovacs, D. A. Scurtu, O. Cadar, A. Becze, M. Senila, M. Roman, D. E. Dumitras and C. Roman, Sustainable biomass pellets production using vineyard wastes, *Agriculture*, 2020, **10**, 1–21.
31 M. Ferrandez-Villena, C. E. Ferrandez-Garcia, T. Garcia-Ortuño, A. Ferrandez-Garcia and M. T. Ferrandez-Garcia, Analysis of the thermal insulation and fire-resistance capacity of particleboards made from vine (*Vitis vinifera* L.) prunings, *Polymers*, 2020, **12**, 1147.
32 I. Lorero, A. J. Vizcaíno, F. J. Alguacil and F. A. López, Activated carbon from winemaking waste: Thermoeconomic analysis for large-scale production, *Energies*, 2020, **13**, 6462.
33 R. Sánchez-Gómez, A. Zalacain, F. Pardo, G. L. Alonso and M. R. Salinas, Moscatel vine-shoot extracts as a grapevine biostimulant to enhance wine quality, *Food Res. Int.*, 2017, **98**, 40–49.
34 C. Bignami, F. Melegari, M. Zaccardelli, C. Pane and D. Ronga, Composted solid digestate and vineyard winter prunings partially replace peat in growing substrates for micropropagated highbush blueberry in the nursery, *Agronomy*, 2022, **12**, 337.
35 M. Wei, T. Ma, Q. Ge, C. Li, K. Zhang, Y. Fang and X. Sun, Challenges and opportunities of winter vine pruning for global grape and wine industries, *J. Cleaner Prod.*, 2022, **380**, 135086.
36 R. Spinelli, N. Magagnotti and C. Nati, Harvesting vineyard pruning residues for energy use, *Biosyst. Eng.*, 2010, **105**, 316–322.
37 S. Paudel and S. Janaswamy, Corncob-derived biodegradable packaging films: A sustainable solution for raspberry post-harvest preservation, *Food Chem.*, 2024, **454**, 139749.
38 S. Regmi and S. Janaswamy, Biodegradable packaging films from the alkali-extracted lignocellulosic residue of soyhulls extend the shelf life of strawberries, *Food Biosci.*, 2025, **65**, 106016.
39 S. Regmi, S. Paudel and S. Janaswamy, Development of eco-friendly packaging films from soyhull lignocellulose: Towards valorizing agro-industrial byproducts, *Foods*, 2024, **13**, 4000.
40 S. Bhattarai and S. Janaswamy, Biodegradable, UV-blocking, and antioxidant films from lignocellulosic fibers of spent coffee grounds, *Int. J. Biol. Macromol.*, 2023, **253**, 126798.
41 S. Bhattarai and S. Janaswamy, Biodegradable, UV-blocking, and antioxidant films from alkali-digested lignocellulosic residue fibers of switchgrass, *Chemosphere*, 2024, **359**, 142393.
42 S. Bhattarai and S. Janaswamy, Biodegradable films from the lignocellulosic residue of switchgrass, *Resour., Conserv. Recycl.*, 2024, **201**, 107322.
43 S. Ahmed, S. Janaswamy and M. P. Yadav, Biodegradable films from the lignocellulosic fibers of wheat straw biomass and the effect of calcium ions, *Int. J. Biol. Macromol.*, 2024, **264**, 130601.
44 S. Ahmed and S. Janaswamy, Green fabrication of biodegradable films: Harnessing the cellulosic residue of oat straw, *Int. J. Biol. Macromol.*, 2025, **303**, 140656.
45 V. D'Eusanio, L. Morelli, A. Marchetti and L. Tassi, Aroma profile of grapevine chips after roasting: A comparative study of sorbara and spergola cultivars for more sustainable oenological production, *Separations*, 2023, **10**, 532.
46 S. O. Prozil, D. V Evtuguin and L. P. C. Lopes, Chemical composition of grape stalks of Vitis vinifera L. from red grape pomaces, *Ind. Crops Prod.*, 2012, **35**, 178–184.
47 Q. Xu, C. Chen, K. Rosswurm, T. Yao and S. Janaswamy, A facile route to prepare cellulose-based films, *Carbohydr. Polym.*, 2016, **149**, 274–281.
48 A. Guleria, A. S. Singha and R. K. Rana, Mechanical, thermal, morphological, and biodegradable studies of okra cellulosic fiber reinforced starch-based biocomposites, *Adv. Polym. Technol.*, 2018, **37**, 104–112.
49 T. Zhou, J. Zhou, Q. Feng, Q. Yang, Y. Jin, D. Li, Z. Xu and C. Chen, Mechanically strong, hydrostable, and biodegradable all-biobased transparent wood films with UV-blocking performance, *Int. J. Biol. Macromol.*, 2024, **255**, 128188.
50 G. Zhao, X. Lyu, J. Lee, X. Cui and W.-N. Chen, Biodegradable and transparent cellulose film prepared eco-friendly from durian rind for packaging application, *Food Packag. Shelf Life*, 2019, **21**, 100345.
51 Z. Fang, H. Zhu, C. Preston, X. Han, Y. Li, S. Lee, X. Chai, G. Chen and L. Hu, Highly transparent and writable wood all-cellulose hybrid nanostructured paper, *J. Mater. Chem. C*, 2013, **1**, 6191–6197.
52 S. Guzman-Puyol, J. J. Benítez and J. A. Heredia-Guerrero, Transparency of polymeric food packaging materials, *Food Res. Int.*, 2022, **161**, 111792.
53 R. Tian, C. Wang, W. Jiang, S. Janaswamy, G. Yang, X. Ji and G. Lyu, Biodegradable, strong, and hydrophobic regenerated cellulose films enriched with esterified lignin nanoparticles, *Small*, 2024, 2309651.
54 S. A. Hussain, M. P. Yadav, B. K. Sharma, P. X. Qi and T. Z. Jin, Biodegradable food packaging films using a combination of hemicellulose and cellulose derivatives, *Polymers*, 2024, **16**, 3171.
55 S. Paudel, S. Regmi and S. Janaswamy, Effect of glycerol and sorbitol on cellulose-based biodegradable films, *Food Packag. Shelf Life*, 2023, **37**, 101090.
56 V. R. Suryavanshi, R. Santhosh, H. Singhi, R. Thakur, J. Ahmed, K. K. Gaikwad, A. S. Kumawat, S. Roy and P. Sarkar, Preparation and characterization of kodo millet starch/gum tragacanth/copper oxide nanoparticles-based antimicrobial food packaging films, *Mater. Today Commun.*, 2025, **42**, 111443.
57 E. R. Rajeshwari, P. S. Sathanya, S. Vignesh, V. Chandrasekar and N. Baskaran, Valorization of Borassus flabellifer sprout peel: Synthesis and characterization of carboxymethyl cellulose for biodegradable packaging, *Biomass Convers. Biorefin.*, 2025, DOI: **10.1007/s13399-025-06500-0**.

58 P. Chakraborty, S. Hati and B. K. Mishra, Preparation and characterization of nanobiocomposite films from sodium caseinate, halloysite nanoclay, and geraniol and application on capsicum (Capsicum annuum) fruits as a case study, *Food Biosci.*, 2024, **61**, 104665.
59 Y. Liu and H.-J. Kim, Fourier transform infrared spectroscopy (FT-IR) and simple algorithm analysis for rapid and non-destructive assessment of developmental cotton fibers, *Sensors*, 2017, **17**, 1469.
60 N. Abidi, L. Cabrales and C. H. Haigler, Changes in the cell wall and cellulose content of developing cotton fibers investigated by FTIR spectroscopy, *Carbohydr. Polym.*, 2014, **100**, 9–16.
61 Q. Ding, W. Han, X. Li, Y. Jiang and C. Zhao, New insights into the autofluorescence properties of cellulose/nanocellulose, *Sci. Rep.*, 2020, **10**, 21387.
62 Y. Kim, D. Jeong, K. H. Park, J.-H. Yu and S. Jung, Efficient adsorption on benzoyl and stearoyl cellulose to remove phenanthrene and pyrene from aqueous solution, *Polymers*, 2018, **10**, 1042.
63 M. Szymańska-Chargot, J. Cieśla, P. Pękala, P. M. Pieczywek, W. Oleszek, M. Żyła, Z. Szkopek and A. Zdunek, The influence of high-intensity ultrasonication on properties of cellulose produced from the hop stems, the byproduct of the hop cones production, *Molecules*, 2022, **27**, 2624.
64 R. M. Salim, J. Asik and M. S. Sarjadi, Chemical functional groups of extractives, cellulose and lignin extracted from native Leucaena leucocephala bark, *Wood Sci. Technol.*, 2021, **55**, 295–313.
65 V. Hospodarova, E. Singovszka and N. Stevulova, Characterization of Cellulosic Fibers by FTIR Spectroscopy for Their Further Implementation to Building Materials, *Am. J. Anal. Chem.*, 2018, **09**, 303–310.
66 W. Kong, M. Chang, C. Zhang, X. Liu, B. He and J. Ren, Preparation of xylan-g-/P(AA-co-AM)/GO nanocomposite hydrogel and its adsorption for heavy metal ions, *Polymers*, 2019, **11**, 621.
67 M. Rabyk, A. Galisova, M. Jiratova, V. Patsula, L. Srbova, L. Loukotova, J. Parnica, D. Jirak, P. Stepanek and M. Hruby, Mannan-based conjugates as a multimodal imaging platform for lymph nodes, *J. Mater. Chem. B*, 2018, **6**, 2584–2596.
68 T. T. T. Nguyen, H. T. Ho, D. Hoang, Q. A. P. Nguyen and T. Van Tran, Novel films of pectin extracted from ambarella fruit peel and jackfruit seed slimy sheath: Effect of ionic crosslinking on the properties of pectin film, *Carbohydr. Polym.*, 2024, **334**, 122043.
69 S. Mukherjee, A. Sengupta, S. Preetam, T. Das, T. Bhattacharya and N. Thorat, Effects of fatty acid esters on mechanical, thermal, microbial, and moisture barrier properties of carboxymethyl cellulose-based edible films, *Carbohydr. Polym. Technol. Appl.*, 2024, **7**, 100505.
70 R. Xu, L. Xia, Q. Tang, F. Tang, S. Pang, H. Li and Z. Zou, High-performance carboxymethyl starch/PVA based intelligent packaging films engineered with Cu-Trp nanocrystal as functional compatibilizer, *Food Chem.*, 2024, **454**, 139696.
71 N. Khotsaeng, W. Simchuer, T. Imsombut and P. Srihanam, Effect of glycerol concentrations on the characteristics of cellulose films from cattail (Typha angustifolia L.) flowers, *Polymers*, 2023, **15**, 4535.
72 A. R. Barman, P. P. Dutta, K. Kapila, K. K. Bania and D. J. Haloi, Synergistic effect of glycerol and calcium chloride on the properties of cellulose acetate film, *J. Appl. Polym. Sci.*, 2025, **142**, e56615.
73 A. Alahmed and S. Simsek, Improving biodegradable films from corn bran arabinoxylan for hydrophobic material and green food packaging, *Foods*, 2024, **13**, 1914.
74 R. Santhosh and P. Sarkar, Fabrication of jamun seed starch/tamarind kernel xyloglucan bio-nanocomposite films incorporated with chitosan nanoparticles and their application on sapota (Manilkara zapota) fruits, *Int. J. Biol. Macromol.*, 2024, **260**, 129625.
75 Z. Wang, Nacre-like structural carboxymethyl cellulose dual-layered film with a combination of high strength, elongation, and UV-blocking for food packaging, *Int. J. Biol. Macromol.*, 2025, **306**, 141692.
76 B. Girgin, M. Abahuni Uçar, E. Moroydör Derun and N. Tugrul, Development of edible packaging films from walnut, mango, and orange peels: Effect of plasticizers and essential oils, *ACS Food Sci. Technol.*, 2025, **5**, 75–84.
77 E. Matta and N. Bertola, Development and characterization of high methoxyl pectin film by using isomalt as plasticizer, *J. Food Process. Preserv.*, 2020, **44**, 14568.
78 P. Sahu and M. K. Gupta, Water absorption behavior of cellulosic fibres polymer composites: A review on its effects and remedies, *J. Ind. Text.*, 2022, **51**, 7480S–7512S.
79 O. N. Pozharitskaya, A. N. Shikov, D. V Demchenko, E. V Flisyuk, V. G. Makarov and S. S. C. Academy, Effect of plasticizers on moisture absorption and mechanical properties of agar films, *Pharmacy*, 2017, **8**, 18–23.
80 D. Turan, Water vapor transport properties of polyurethane films for packaging of respiring foods, *Food Eng. Rev.*, 2021, **13**, 54–65.
81 M. Giacinti Baschetti and M. Minelli, Test methods for the characterization of gas and vapor permeability in polymers for food packaging application: A review, *Polym. Test.*, 2020, **89**, 106606.
82 R. Bhat, N. Abdullah, R. H. Din and G.-S. Tay, Producing novel sago starch based food packaging films by incorporating lignin isolated from oil palm black liquor waste, *J. Food Eng.*, 2013, **119**, 707–713.
83 N. N. T. Tien, H. T. Nguyen, N. L. Le, T. T. Khoi and A. Richel, Biodegradable films from dragon fruit (Hylocereus polyrhizus) peel pectin and potato starches crosslinked with glutaraldehyde, *Food Packag. Shelf Life*, 2023, **37**, 101084.
84 L. Marangoni Júnior, R. G. da Silva, R. P. Vieira and R. M. V. Alves, Water vapor sorption and permeability of sustainable alginate/collagen/SiO_2 composite films, *Lebensm.-Wiss. Technol.*, 2021, **152**, 112261.
85 C. d. L. Barizão, M. I. Crepaldi, O. d. O. S. Junior, A. C. de Oliveira, A. F. Martins, P. S. Garcia and E. G. Bonafé, Biodegradable films based on commercial κ-carrageenan

and cassava starch to achieve low production costs, *Int. J. Biol. Macromol.*, 2020, **165**, 582–590.

86 R. R. Koshy, A. Reghunadhan, S. K. Mary, S. Sadanandan, S. Jose, S. Thomas and L. A. Pothen, AgNP anchored carbon dots and chitin nanowhisker embedded soy protein isolate films with freshness preservation for active packaging, *Food Packag. Shelf Life*, 2022, **33**, 100876.

87 M. Soofi, A. Alizadeh, H. Hamishehkar, H. Almasi and L. Roufegarinejad, Preparation of nanobiocomposite film based on lemon waste containing cellulose nanofiber and savory essential oil: A new biodegradable active packaging system, *Int. J. Biol. Macromol.*, 2021, **169**, 352–361.

88 S. Mohan and K. Panneerselvam, A short review on mechanical and barrier properties of polylactic acid-based films, *Mater. Today: Proc.*, 2022, **56**, 3241–3246.

89 Y. Li, Q. Duan, S. Yue, M. Alee and H. Liu, Enhancing mechanical and water barrier properties of starch film using chia mucilage, *Int. J. Biol. Macromol.*, 2024, **274**, 133288.

90 Z. Jaderi, F. Tabatabaee Yazdi, S. A. Mortazavi and A. Koocheki, Effects of glycerol and sorbitol on a novel biodegradable edible film based on Malva sylvestris flower gum, *Food Sci. Nutr.*, 2023, **11**, 991–1000.

91 S. M. Gonçalves, D. C. dos Santos, J. F. G. Motta, R. R. dos Santos, D. W. H. Chávez and N. R. de Melo, Structure and functional properties of cellulose acetate films incorporated with glycerol, *Carbohydr. Polym.*, 2019, **209**, 190–197.

92 A. Sood and C. S. Saini, Red pomelo peel pectin based edible composite films: Effect of pectin incorporation on mechanical, structural, morphological and thermal properties of composite films, *Food Hydrocolloids*, 2022, **123**, 107135.

93 C. Lalnunthari, L. M. Devi and L. S. Badwaik, Extraction of protein and pectin from pumpkin industry by-products and their utilization for developing edible film, *J. Food Sci. Technol.*, 2020, **57**, 1807–1816.

94 M. Jridi, O. Abdelhedi, A. Salem, H. Kechaou, M. Nasri and Y. Menchari, Physicochemical, antioxidant and antibacterial properties of fish gelatin-based edible films enriched with orange peel pectin: Wrapping application, *Food Hydrocolloids*, 2020, **103**, 105688.

95 P. Rodsamran and R. Sothornvit, Microencapsulation of Thai rice grass (O. Sativa cv. Khao Dawk Mali 105) extract incorporated to form bioactive carboxymethyl cellulose edible film, *Food Chem.*, 2018, **242**, 239–246.

96 L. Bastarrachea, S. Dhawan and S. S. Sablani, Engineering properties of polymeric-based antimicrobial films for food packaging, *Food Eng. Rev.*, 2011, **3**, 79–93.

97 M. Julinová, L. Vaňharová, M. Jurča, A. Minařík, P. Duchek, J. Kavečková, D. Rouchalová and P. Skácelík, Effect of different fillers on the biodegradation rate of thermoplastic starch in water and soil environments, *J. Polym. Environ.*, 2020, **28**, 566–583.